



ELSEVIER

Nuclear Instruments and Methods in Physics Research A 455 (2000) 759–768

**NUCLEAR
INSTRUMENTS
& METHODS
IN PHYSICS
RESEARCH**
Section A

www.elsevier.nl/locate/nima

A fast beam position monitor based on arrays of secondary emission monitors

M. Steinacher*, I. Sick

Department of Physics and Astronomy, University of Basel, Klingelbergstr. 82, 4056 Basel, Switzerland

Received 3 May 2000; accepted 4 May 2000

Abstract

We describe an instrument for a fast determination of the beam position of a rastered high-energy electron beam with an intensity as low as 10 nA. Two arrays of stripes of thin metal foils, one in the horizontal and one in the vertical direction, are inserted into the beam. They work as a position-sensitive Secondary Emission Monitor (SEM) with a resolution of 1 mm. The charges from the stripes are amplified and converted into position signals using electronics providing a low vibration sensitivity and a fast beam position measurement. At a beam intensity of 10 nA a measurement can be carried out with an integration time of only 130 μ s. © 2000 Elsevier Science B.V. All rights reserved.

Keywords: Secondary emission monitor; Target beam position monitor; Vibration sensitivity; Gated differential integrator; Raster; Polarized target; Interpolation

1. Introduction

In scattering experiments using a high-energy polarized electron beam and a polarized target in particular it is common to raster the beam over the target. The raster covers an area of several cm^2 and prevents the polarized target from depolarizing due to local heating [1]. The rastering is performed by electromagnets supplied by appropriate alternating currents [2]. Separate electromagnets are used for the horizontal and vertical deflection. Depending on the drive parameters of the deflection-magnets (frequency, amplitude, phase), different raster-patterns such as spiral or TV-scan can be achieved.

The corresponding speed of the beam-spot on the target is in the order of several m/s. Therefore a standard Beam Position Monitor (BPM) [3] cannot be used because it has a response time of several 100 ms at low beam currents and the accuracy deteriorates for beam currents below 100 nA [4].

For a precise reconstruction of the kinematics for a scattering event, the interaction point of the beam at the target must be known. An approach often used involves a static calibration of the deflection-magnet current with a standard BPM right in front of the target. While rastering, the beam position on the target is calculated from the actual currents in the deflection magnets using the calibration parameters. During the calibration procedure the target has to be removed from the beam. This approach suffers from limited accuracy due to magnetic hysteresis and a poor long time stability due to thermal effects. The calibration must be repeated if any

*Corresponding author. Tel.: +41-61-267-3722; fax: +41-61-267-3784.

E-mail address: michael.steinacher@unibas.ch (M. Steinacher).

parameters such as beam energy, target angle, etc., have been changed.

To increase the reliability and accuracy of the beam position measurement, we have developed and installed a Target-BPM (TBPM) in front of the polarized target used in hall C at Thomas Jefferson National Accelerator Facility (TJNAF). It is capable of determining the actual beam position within a short integration time. The TBPM, containing 28 sensitive stripes of 1 mm width, allows a measurement of the beam position for each trigger with a resolution of 1 mm; as a consequence the interaction point between the electron beam and the polarized target is known for each event. If a linear beam movement (TV-scan) is used for rastering, a position resolution better than 1 mm can

be achieved by selecting a integration time equal to a beam travel during 1 mm. The charge interpolation between the two hit metal stripes then results in a more accurate beam position. At a beam current of 10 nA, assuming a secondary electron emission coefficient of 2%, the TBPM has a minimum integration time of 130 μ s. At higher beam currents the minimum integration time is correspondingly shorter.

2. Pick-up

The measurement principle of the TBPM is based on Secondary Electron Emission (SEE) [5] induced by the penetrating high-energy

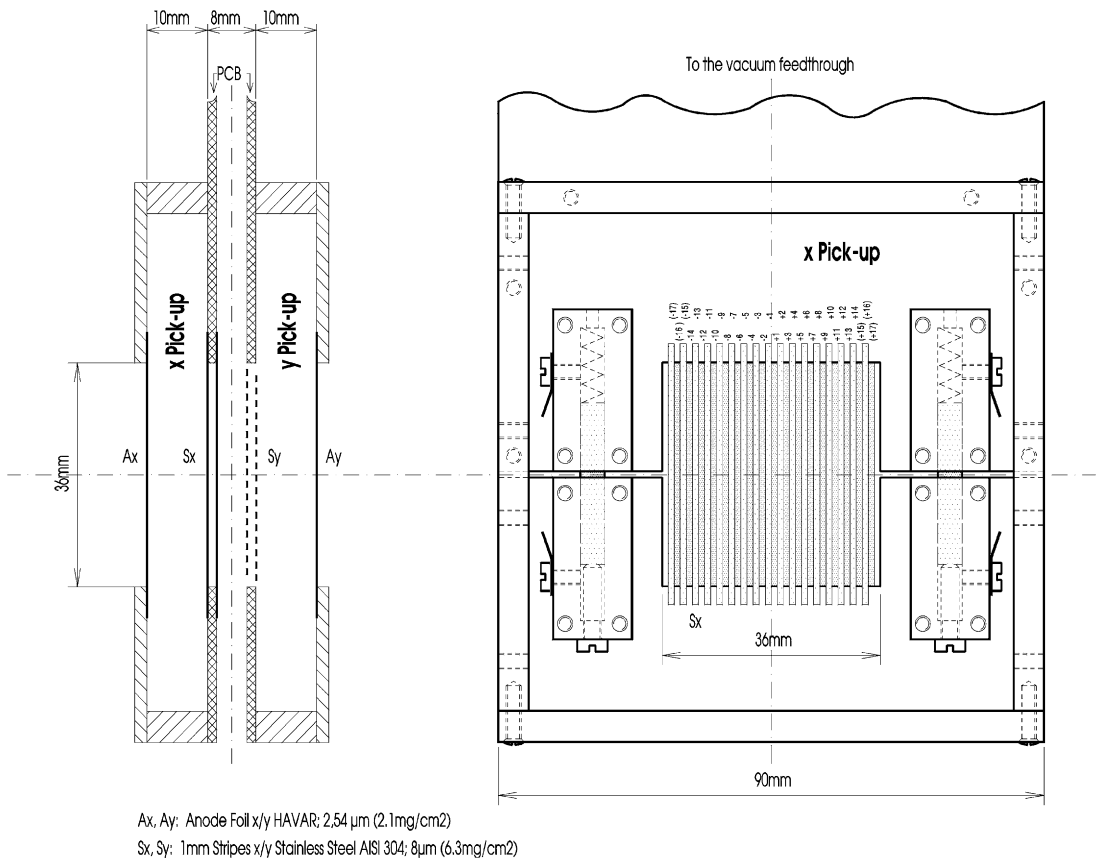


Fig. 1. Left: vertical cross-section through the inner part of the TBPM. The horizontal and vertical pick-up are face to face and the electron beam passes the pick-up from left to right. Right: front-view on the x pick-up (horizontal axis) with removed anode foil and aluminum mounting plate. Left and right of the stripe-array a spring mechanism ensures that the stripes are always tight.

electron-beam on the horizontal and the vertical metal stripe-arrays. Each plane consists of 34 stainless-steel stripes (AISI 304) [6] with a width of 1 mm and a thickness of $8\ \mu\text{m}$ ($6.3\ \text{mg}/\text{cm}^2$). The two ends of the stripes are glued with a conductive glue on the gold-pads of a cut out Printed Circuit Board (PCB). In order to cover the entire area with stripes, the odd-numbered stripes are glued on the top and the even-numbered stripes on the bottom of the PCB (see Fig. 1). Therefore, the odd- and even-numbered stripes are spaced by the thickness of the PCB (1.6 mm) in beam direction. To simplify the positioning and mounting of the stripes to the PCB a patch of 17 parallel stripes spaced by 1 mm is processed at once. The patches are manufactured by LASER-cutting 18 slits (1 mm width; 1 mm spacing; 42 mm height) in a stainless steel foil with the dimensions of $50\ \text{mm} \times 50\ \text{mm}$. The surplus foil around the slits forms a supporting frame for the 17 stripes. After exactly positioning and fixing the patch onto the PCB the supporting frame is cut.

The right side of Fig. 1 shows a front view on the PCB of the horizontal direction (x -axis). It is cut into two parts interconnected by a spring mechanism to ensure that the stripes are always kept tight. For each direction only 28 of the total 34 stripes are read out, corresponding to a coverage of $\pm 14\ \text{mm}$ in both directions.

The anode foils on both sides of the stripe-arrays are used to collect the backward secondary electrons from the x -axis and the forward secondary electrons from the y -axis. The anode foils are also glued with a conductive glue on an aluminum plate with an opening of $36\ \text{mm} \times 36\ \text{mm}$. The anode foils are made of $2.54\ \mu\text{m}$ ($2.1\ \text{mg}/\text{cm}^2$) HAVAR [7]. An anode voltage of $+100\ \text{V}$ is applied and a homogenous electric field of $100\ \text{V}/\text{cm}$ is formed between the stripe-arrays and the collecting anodes. On both pick-up's the anode voltage is filtered by a RC low pass filter; the anode foils with the aluminum mounting frames provide an excellent electrical shielding for the very sensitive stripe-arrays.

The inner part of the TBPM pick-up is mounted in a vacuum-can with two flanges for the connection to the beam pipe and one flange (top) for the vacuum feedthrough of the pick-up signals. A below supported by three threaded rods allows to adjust the inner part in the vertical direction within

$\pm 20\ \text{mm}$ (see Fig. 2). This vertical adjustment is needed for the alignment of the TBPM according to the deflection of the electron beam by the strong magnetic field of the polarized target. Since magnetic fields up to 1 T can be present at the location of the TBPM, it is made entirely from non-magnetic materials.

3. Signal processing

At a beam intensity of 10 nA the Secondary Electron Emission (SEE) current on a hit metal stripe is only about 200 fA. Therefore the SEE current has to be integrated over a certain time. This is realized in the so-called Gated Differential Integrator (GDI) controlled by the gate signal from the Timing Unit (TU). Due to the necessary high charge sensitivity the GDIs have to be installed as close as possible to the TBPM pick-up. They are housed in two well shielded boxes on top of the vacuum can (see Fig. 2). Due to the differential input, each GDI processes two stripes in parallel. It measures the charge difference of two stripes equally spaced from the center of the pick-up (see Fig. 3). This layout results in a noise reduction and a low-vibration sensitivity because all signals affecting both stripes

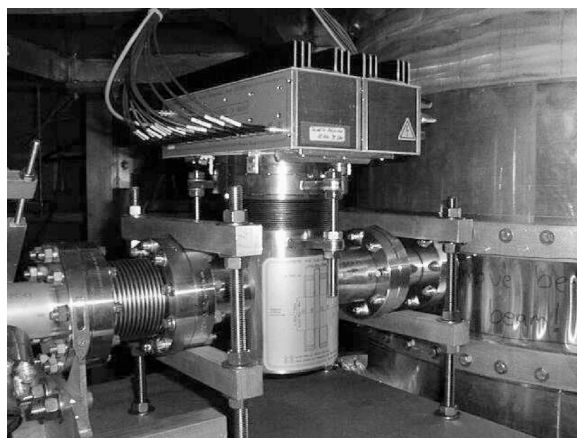


Fig. 2. The TBPM installed in front of the polarized target used in hall C at TJNAF. The beam arrives from the left, passes the pick-up and enters into the target-chamber on the right. The TBPM pick-up is housed in the vacuum-can and the two Gated Integrator Boxes are installed on the top.

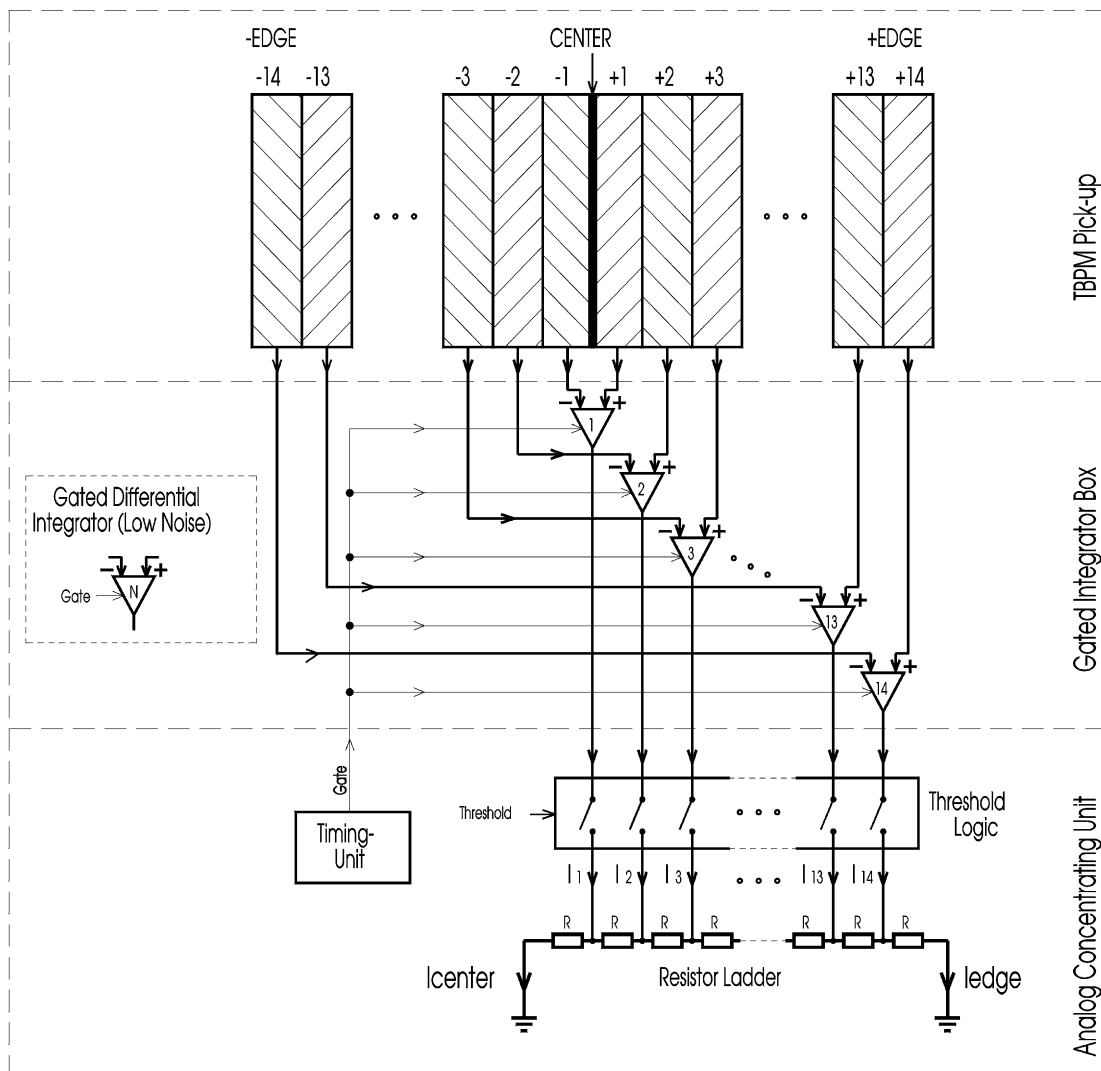


Fig. 3. The simplified layout of the signal processing from the pick-up to the position-currents I_{center} and I_{edge} . The three blocks TBPM Pick-up, Gated Integrator Box, Analog Concentrating Unit are physically separated: The Gated Integrator Box is installed on top of the TBPM and the Analog Concentrating Unit is separated by 50Ω cables several meters from the Gated Integrator Box.

in common are cancelled out. The GDI integrates the charge difference and converts it to a proportional bipolar output current, capable to drive a 50Ω load. A positive GDI output current indicates that more charge was integrated on the positive stripe than on the negative and vice versa.

The 14 output currents of the GDIs are connected to the Threshold Logic (TL) which selects the currents over a given threshold for further process-

ing; the noise-currents of all other GDIs are suppressed. Only the selected currents are injected in the Resistor Ladder (RL) consisting of 15 identical precision resistors. The RL has a twofold function: It allows to interpolate between the signals from different stripes. At the same time it concentrates the position information into two signals (I_{center} , I_{edge}) which can easily be fed to the data-acquisition system of the main experiment.

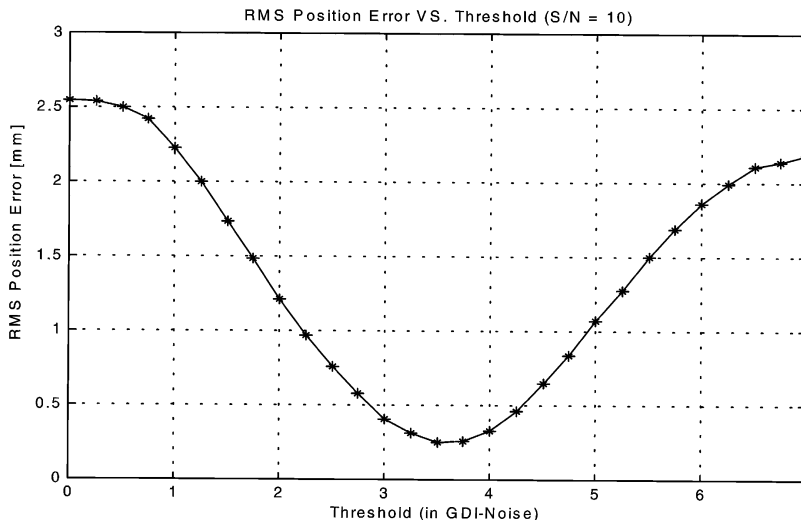


Fig. 4. Monte-Carlo simulation of the mean RMS position error versus the threshold. The interpolated position error drops by more than a factor of eight by setting a threshold of four times the GDI-noise (RMS value). High thresholds restrict the interpolation facility of the TBPM.

The Monte-Carlo simulation of the RMS position error versus the threshold is presented in Fig. 4. The threshold is given in terms of the GDI-noise (RMS value). For an optimal interpolation an integration time equal to a beam travel during 1 mm is assumed in the simulation. The signal-to-noise ratio (S/N) is defined as: Output current of the GDI after the integration time, divided by the RMS current-noise of the GDI. The simulation is made with a S/N of 10, typical for such short integration times. The optimal threshold is around 4 times the GDI-noise and this optimum is independent of the S/N .

Because the GDIs have a bipolar-current output the threshold is symmetrical for positive and negative current outputs. After the integration time only currents reaching the threshold are injected into the RL. According to the equation below the beam position can be calculated from the two currents I_{center} and I_{edge} independent of the beam intensity.

$$\text{beam position} = \frac{15I_{\text{edge}}}{|I_{\text{edge}} + I_{\text{center}}|}$$

The beam position is equal to the stripe number from -14 to $+14$ omitting position '0'. A beam

spot precisely at the center of the pick-up results in I_{edge} and I_{center} equal to zero, due to the charge canceling at the GDI 1.

4. Gated differential integrator

The SEE currents (I_e) on all stripes of one axis are synchronously integrated in the Gated Integrator Box (GIB). Two GIBs, one for each axis, are mounted on top of the TBPM. The integration times are controlled by two different gate signals for the x - and y -axis. Both gate signals are activated synchronously, but the duration for the two axis may be different. This gives the flexibility to cope with different rastering schemes.

The two GIBs are directly plugged into the vacuum feedthrough connectors and can be easily removed for service purposes. The x - and y -axis have their own well isolated GIB holding the 14 Gated Differential Integrators (GDI) in slot technique, optimal for maintenance. During a high gate signal the analog switches SW1 and SW2 are open and the SEE currents of the positive and negative stripe are integrated on two separate integrators (see Fig. 5). The GDI inputs are protected against

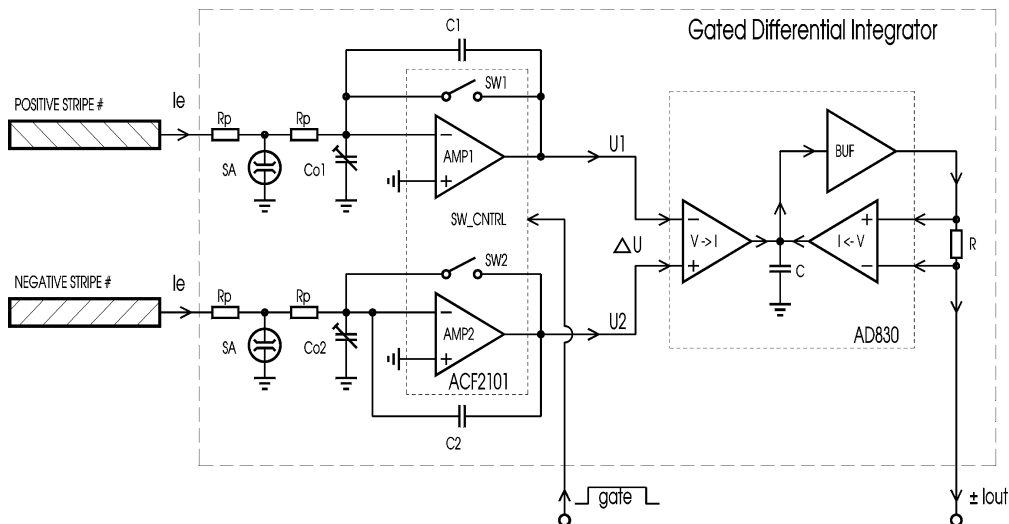


Fig. 5. The basic circuit diagram of the GDI. 28 such GDIs are used for the TBPM. The first stage includes two low noise gated integrators both synchronously controlled by the gate signal. The second stage converts the voltage difference ΔU to the bipolar output current $\pm I_{out}$.

high-voltage discharge using gas-filled (high impedance) Surge Arresters (SA) and current-limiting resistors (R_p).

The charge integration is realized with the Low Noise, Dual Switched Integrator chip ACF2101 [8,9] from Burr-Brown. To get a reasonable output voltage, external integration capacitors (C_1 , C_2) of only 1 pF are used. These are very stable capacitors and they are matched to reach a maximum common mode rejection. Due to the charge transfer [10], occurring upon opening the analog switches SW1 and SW2, the output voltages U_1 and U_2 make a step upon start of the integration. Because both switches are on the same chip the charge transfers to C_1 and C_2 are similar and the temperature dependence is the same. Nevertheless, the two trim capacitors Co_1 and Co_2 must be adjusted to ensure that the integration starts at a voltage difference ($\Delta U = U_1 - U_2$) of exactly zero.

The voltage difference (ΔU) is converted to a bipolar output current ($\pm I_{out}$) capable to drive a $50\ \Omega$ load using a Video Difference Amplifier chip AD830 [11–13] from Analog Devices.

A charge difference of 25 fC (corresponding to 156 000 electrons) is converted by the GDI to an output current of 10 mA. After an integration time of 130 μ s the GDI has a typical output current

noise of 1 mA_{RMS}, measured in the laboratory. The GDI is saturated at an output current of about ± 100 mA, which corresponds to 250 fC. As long as the interpolation facility is not used, the saturation of the GDI does not affect the determination of the beam position. The 28 output currents of the x - and y -axis are fed to the Analog Concentrating Unit (ACU) for further processing. The ACU also generates the two separate gate signals for the x - and y -axis.

5. General layout

The complete electronics of the TBPM [14] consists of the two Gated Integrator Boxes (GIBs) and the Analog Concentrating Unit (ACU). The position measurement is initiated by the trigger signal of the main experiment. The ACU consists of two identical parts for the x - and y -axis. Fig. 6 shows the block diagram of the electronics needed for the x -axis. The ADCs, located in the counting room and triggered by the Start ADC signals, register the position signals.

The three main parts of the ACU are:

- The Threshold Logic & Display Unit (TLDU) receives the 14 output currents of the GDI and

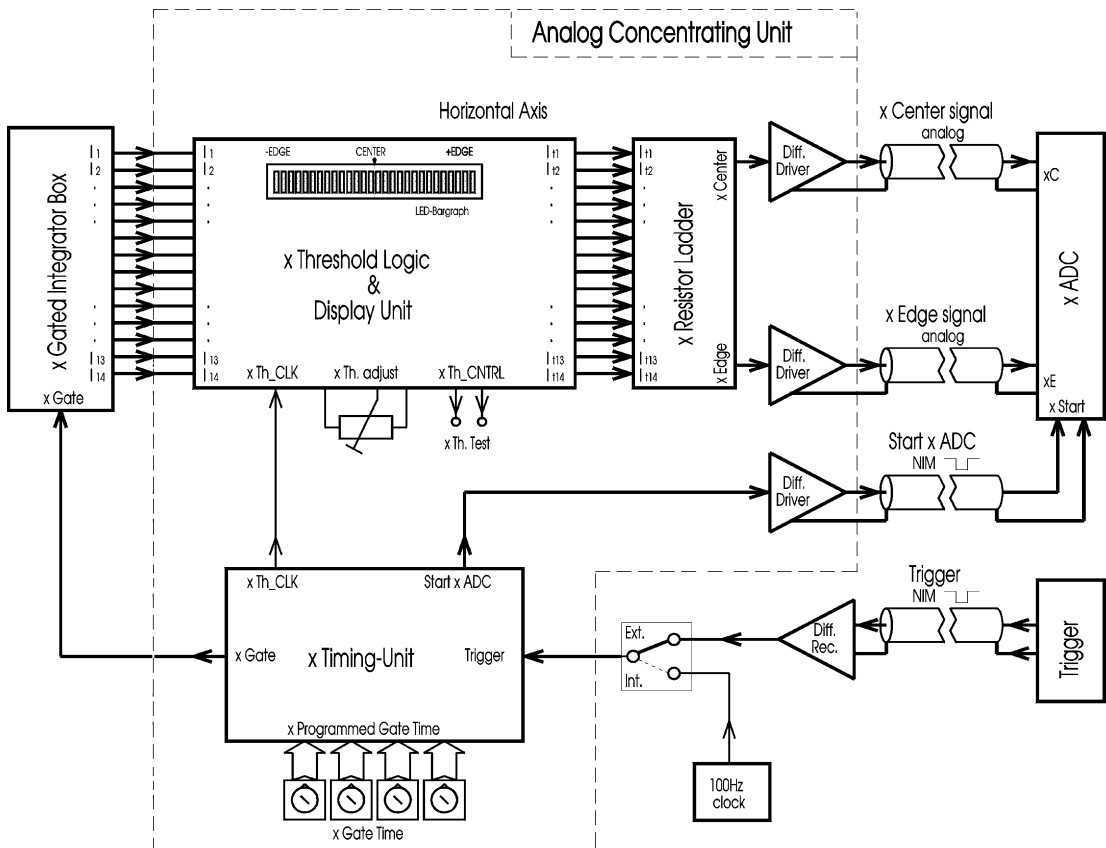


Fig. 6. The block diagram of the electronics needed for the x-axis. The ADCs and the trigger electronics are located in the counting room.

selects only the signals above the adjusted threshold for further processing. At the end of the integration time, indicated by the Th_CLK signal, all channels over the threshold are displayed on a LED-bargraph. This is useful for a coarse-beam position reading.

- The selected currents of the TLDU are added by the Resistor Ladder (RL) to the two-position-dependent signals Center and Edge. To reduce ground-loop problems these analog signals are sent to the ADC in the counting room via differential current drivers. The analog signals are turned on $2 \mu\text{s}$ before the Start ADC signal and turned off $1 \mu\text{s}$ after the Start ADC signal. During all this time the GDIs are in the integration mode.
- The Timing Unit (TU) receives the Trigger signal from the trigger electronics in the counting

room. It starts the integration with the preset Gate Time (GT) and ends with the Start ADC signal. The GT is programmable by four HEX-switches with a resolution of 100 ns. The minimum GT is limited to $15 \mu\text{s}$ by the initial settling-time of the GDIs; the maximum GT is 6.55 ms. A typical GT during normal operation is in the range from 20 to $200 \mu\text{s}$. The minimum time between two measurements of $4 \mu\text{s}$ is given by the reset-time of the GDIs. The ACU can be triggered either by an external Trigger or internal 100 Hz clock. The Trigger signal is common for both x- and y-axis.

The values of the ADCs are read by the data acquisition system and the beam position at the trigger-time can be calculated offline from these ADC-values. Events with a Center- and an

Edge-signal equal to zero have to be further analyzed: They can come from a beam position at the center due to charge-canceling at the GDI 1 or from an event with no beam. Therefore the beam on/off information has to be integrated in the calculation of the beam position.

6. Measurements

The following measurements were made in hall C at TJNAF during the G_{en} experiment. The beam current varied between 50 and 200 nA and all the data were taken at a beam energy of 2.7 GeV.

A large Slow Raster (SR) spiral superimposed with a small Fast Raster (FR) spiral is used to prevent the polarized target from locally overheating and depolarizing. The SR has a typical diameter of 20 mm, a spin frequency of 117 Hz and the time from the center to the outside of the spiral amounts to 0.85 s. The FR has a typical diameter of 1 mm, a spin frequency of 24 kHz and an expansion time of 4.25 ms. Both rasters can be switched on and off and the nominal diameter can be set individually.

Due to the variable beam-spot speed of the SR-spiral, depending on the actual diameter, no optimal integration time for interpolation can be specified. Nevertheless, with the FR on, the beam may hit more than one stripe and the interpolation facility of the TBPM is enabled. The probability of hitting more than one stripe depends on the diameter of the FR-spiral at the time of the measurement. In order to avoid an increase in dead-time of the data acquisition, an integration time of 40 μ s is selected. This corresponds to the time of one revolution of the FR-spiral. With this integration time the TPBM works down to a beam current of about 35 nA. The threshold of the ACU is set to 300 mV, corresponding to four times the RMS-noise of the installed GDI. In the beam pipe, the GDI-noise is about 50% higher than the noise measured in the laboratory. It is mainly induced by vibrations of the beam-pipe.

The following plots show the two-dimensional view of the measured beam position in a range of ± 15 mm for both axes; each event is represented by a dot. Since the metal stripes of the pick-up have a width of 1 mm, the geometrical center of the

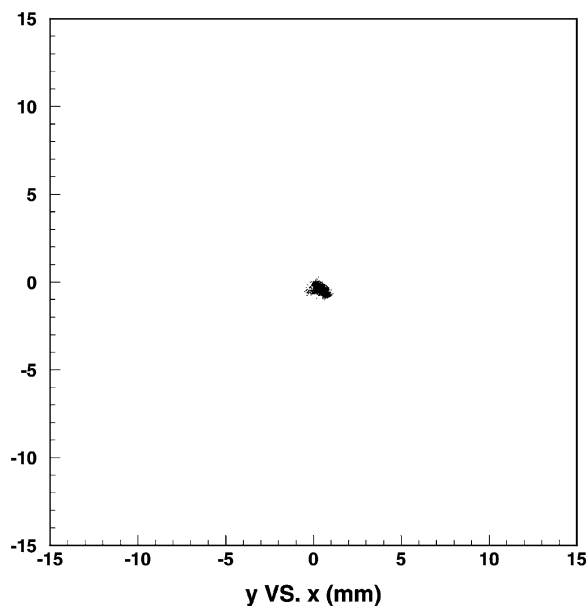


Fig. 7. TBPM measurement with no raster at a nominal centered beam position and a beam current of 168 nA.

calculated stripe number represents directly the beam position in millimeters. For example, the stripe number + 1 corresponds to a beam position of +0.5 mm and the stripe number -1 to -0.5 mm.

Fig. 7 shows the x - y plot of about 3000 events of an unrastered beam with an intensity of 168 nA. The nominal beam position is set to the center, using a standard BPM with a long integration time. The reading of the TBPM shows that the beam position is about half a millimeter low and shifted by half a millimeter to the right. The size of the spot indicates that the beam position drifted slightly during the run.

Fig. 8 shows the x - y plot of about 20 000 events of a rastered beam with an intensity of 66 nA. Only the SR-spiral with a diameter of 20 mm is turned on and thus the interpolation facility of the TBPM is curtailed. The amass of points in a grid of 1 mm is due to the intrinsic 1 mm resolution of the TBPM if no interpolation can be made.

A measurement, consisting of 20 000 events, with a SR-spiral as well as a FR-spiral at a beam current of 158 nA is shown in Fig. 9. The SR-spiral has

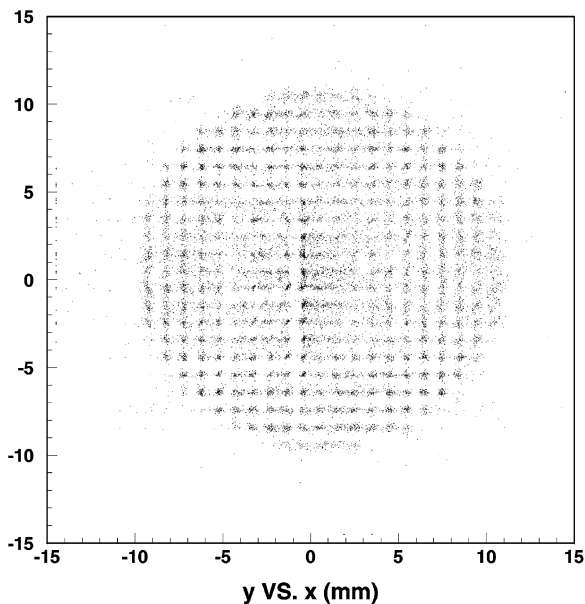


Fig. 8. TBPM measurement with a SR-spiral with a diameter of 20 mm at a beam current of 66 nA.

a diameter of 20 mm and the FR-spiral has a diameter of 1 mm. Due to the FR-spiral, the interpolation is more likely and the beam-position measurement is smeared over the circular area of the large SR-spiral. This TBPM measurement shows that the center of the rastered beam was shifted about 1 mm up and 1 mm to the right.

Figs. 8 and 9 show a few points outside of the SR-spiral. This is due to the GDI-noise which potentially reaches the threshold and falsifies the beam position measurement. The true beam position of such events can be reconstructed by using the values of the deflection-magnet currents, calibrated with the TBPM measurements. As this calibration is continuously updated, it does not suffer from drift problems.

7. Summary and conclusion

In this article we have described an instrument for an accurate and ‘real-time’ beam position measurement of a rastered low-current electron beam. A SEM pick-up made of two orthogonal

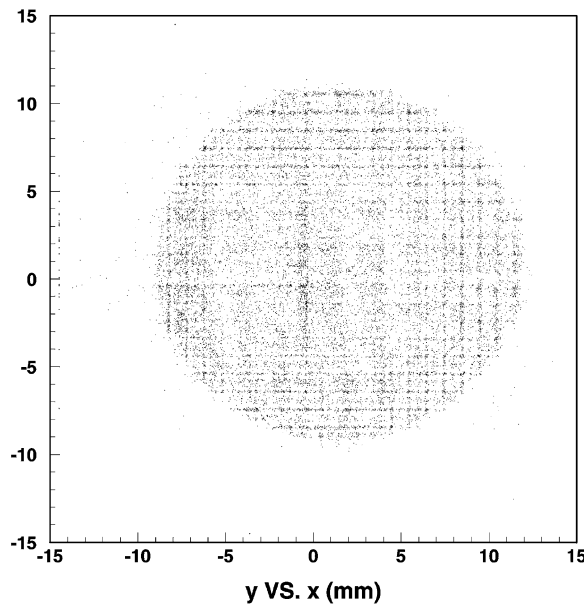


Fig. 9. TBPM measurement with a SR- and FR-spiral at beam current of 158 nA. The SR (FR)-spiral has a diameter of 20 mm (1 mm).

arrays of thin metal stripes is installed in front of the target. The charges on the metal stripes are integrated with gated integrators. The layout of pick-up in common with the dedicated electronics results in low noise and low vibration sensitivity. Even at low signal-to-noise ratios a precise and reliable beam position measurement is possible. The instrument concentrates the beam position information to four analog signals (two for each axis), easy to integrate in an existing data acquisition system. The instrument has been successfully used in an polarized target experiment at TJNAF.

Acknowledgements

The authors would like to thank B. Vulcan, M. Zeier and B. Zihlmann for the support during the installation, the commissioning and the data analysis. This work was supported by the ‘Schweizerischer Nationalfonds’.

References

- [1] T.D. Averett et al., *Nucl. Instr. and Meth. A* 427 (1999) 440.
- [2] J. Beaufait, *Beam Raster*, preprint TJNAF, February 7, 2000.
- [3] W. Barry, *Nucl. Instr. and Meth. A* 301 (1991) 407.
- [4] T. Powers, Improvement of the noise figure of the CEBAF switched electrode electronics BPM system, Proceedings of the 1998 Beam Instrumentation Workshop, Stanford, CA, May 1998, p. 256.
- [5] H. Bruining, *Physics and Applications of Secondary Electron Emission*, Pergamon Press, Oxford, 1954.
- [6] Catalogue, Goodfellow, 1998/1999, p. 341.
- [7] Catalogue, Goodfellow, 1998/1999, p. 303.
- [8] Linear Products, Burr Brown, 1996/1997, 7.5.
- [9] Application Seminar, Burr Brown, 1991, II/20.
- [10] P. Horowitz, W. Hill, in: *The Art of Electronics*, 2nd Edition, Cambridge University Press, Cambridge, 1989, p. 148.
- [11] Designer's Reference Manual, Analog Devices, 1996, 10–69.
- [12] System Applications Guide, Analog Devices, 1993, 11–27.
- [13] C. Naumann, Ideas for Design, *Electronic Design*, March 6, 1995.
- [14] M. Steinacher, TBPM User's Manual, Internal Report, University of Basel, July 3, 1998.